

Reconfigurable Photonic Generation of Binary Modulated Microwave Signals

Volume 12, Number 6, December 2020

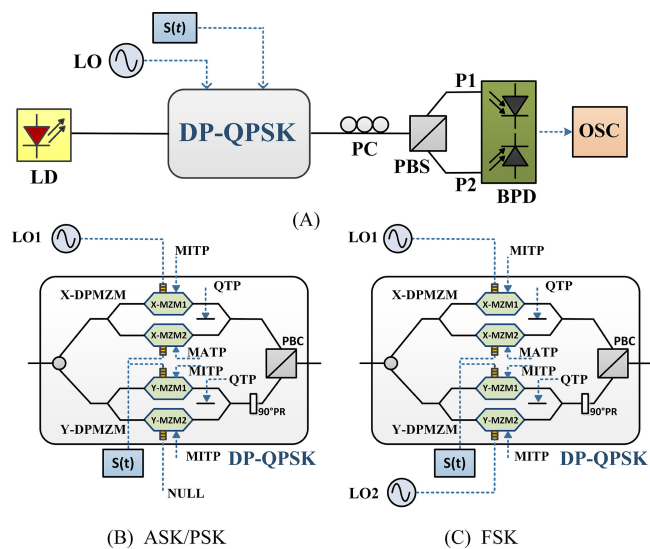
Jialin Ma

Aijun Wen, *Senior Member, IEEE*

Zhaoyang Tu

Xiangjuan Cheng

Yong Wang



DOI: 10.1109/JPHOT.2020.3037793

Reconfigurable Photonic Generation of Binary Modulated Microwave Signals

Jialin Ma,^{1,2} Aijun Wen ,^{1,2} *Senior Member, IEEE*,
Zhaoyang Tu ,^{1,2} Xiangjuan Cheng,^{1,2} and Yong Wang ,^{1,2}

¹State Key Laboratory of Integrated Service Networks, Xidian University, Xi'an 710071, China

²Collaborative Innovation Center of Information Sensing and Understanding, Xidian University, Xi'an 710071, China

DOI:10.1109/JPHOT.2020.3037793

This work is licensed under a Creative Commons Attribution-NonCommercial-NoDerivatives 4.0 License. For more information, see <https://creativecommons.org/licenses/by-nc-nd/4.0/>

Manuscript received October 19, 2020; revised November 6, 2020; accepted November 9, 2020. Date of publication November 16, 2020; date of current version December 9, 2020. This work was supported in part by the National Key Research and Development Program of China under Grant 2017YFB1104800, in part by the National Natural Science Foundation of China under Grant 61674119, in part by the National Postdoctoral Program for Innovative Talents in China under Grant BX201600118, in part by the Young Talent Fund of University Association for Science and Technology in Shaanxi, China under Grant 20160109, Project funded by the China Postdoctoral Science Foundation under Grant 2017M613072, in part by Natural Science Basic Research Plan in Shaanxi Province of China under Grant 2017JM6002, in part by the Key Research and Development Program from Government of Shaanxi Province under Grant 2020GY-009, and in part by National Stability Support Fund under Grant 2018SSFNKLSMT-16. Corresponding author: Aijun Wen (e-mail: ajwen@xidian.edu.cn).

Abstract: A novel photonic scheme of binary modulated microwave signals generation based on a dual-polarization quadrature phase-shift keying (DP-QPSK) modulator is proposed and experimentally demonstrated. The scheme is highly reconfigurable, amplitude keying signal (ASK), phase-shift keying signal (PSK) or frequency-shift keying (FSK) signal can be generated by appropriately setting the amplitude of the binary coding signal. The coding signal and local oscillator (LO) signals are independent with each other, binary modulated microwave signals can be generated with arbitrary coding rate and carrier frequency. The frequency deviation of the FSK signal can also be adjusted flexibly. No filter is used in the scheme and the tuning range is large. A proof-of-concept experiment is carried out to verify the feasibility of the proposed system. A 1-Gbps 8-GHz microwave ASK signal, a 0.5-Gbps 6-GHz microwave PSK signal, and a 0.5-Gbps 8/12-GHz microwave FSK signal are generated in the experiment.

Index Terms: Microwave photonics, Microwave signals generation, binary digitally modulated signals.

1. Introduction

Digital-modulation signals such as amplitude shift keying (ASK), frequency shift keying (FSK), and phase shift keying (PSK) signals are widely used in communications and radar system [1], [2]. Conventional methods to generate ASK / PSK / FSK signal in electric domain are limited by the electric bottleneck. Microwave photonic technique can be used to solve the problem. It has significant advantages, such as large bandwidth, high coding rate and anti-electromagnetic interference [3], [4]. Meanwhile, it can reduce the complexity of the signal generation system.

Various methods have been proposed to generate ASK, PSK and FSK signals in optical domain. Typically, they are divided into three categories, direct space-time mapping, frequency-time

mapping and optical external modulation. Direct space-to-time mapping [5] can flexibly generate a variety of RF binary modulated signals, but the structure is bulky and lossy. For the schemes based on frequency-to-time mapping [6], the duration of the generated signal is affected by dispersion. Schemes based on optical external modulation [7]–[18] can better alleviate the above problems, it has received more and more attention in recent years. For example, the ASK signal can be generated using a Mach-Zehnder modulator (MZM) [7] or a mode-locked laser (MLL) and filters [8]. PSK signal can be generated by using a dual-drive Mach-Zehnder modulator (DDMZM) and optical bandpass filter (OBPF) [9]. In [10], the PSK signal generator is implemented based on a polarization division multiplexing Mach-Zehnder modulator (PDM-MZM) and a 90° hybrid coupler (90° HC). However, in these schemes an OBPF or a 90° HC is used, and the frequency of the generated PSK signal is limited by the OBPF or the 90° HC. In order to increase the operating bandwidth, cascaded structures [11], [12] were proposed. In these schemes, the generation of PSK signals is based on a polarization modulator (PolM), which has two orthogonal polarization states and the modulation indexes are opposite. To reduce the complexity of the scheme, approach based on quadrature phase shift keying modulator (QPSK) is proposed to generate PSK signal [13].

FSK signal generation schemes were proposed in [14]–[16]. In [14], a complex structure with two laser diodes (LD), two modulators (MZM, PolM), and a PM-FBG are used, the stability and tuning range of the system is limited by its PM-FBG and the carrier frequency stability of the system is affected by two incoherent lasers. To simplify the complexity of the system, the coding signal and the LO signal are loaded on a DDMZM in [15], but the generated FSK signal is limited by the frequency doubling relationship. In order to realize better frequency adjustability of the generated FSK signal, scheme [16] is proposed. In this scheme, two independent microwave signals are used as the subcarriers of the FSK signal.

However, most of the mentioned schemes [7]–[16] can only implement one modulation format. Only a few schemes are capable of generating multiple binary modulated microwave signal formats. A binary digital modulated signal generation scheme is proposed in [17], which includes a PolM, two parallel Mach-Zehnder interferometers (MZI), and a tunable optical filter (TOF). Different modulation formats can be generated by adjusting an optical delay line and an optical switch. Similarly, the scheme in ref. [18] is composed of an optical comb generator, a PM, an MZI and a TOF. Different modulation formats can be generated by adjusting the MZI and the TOF. The tunability of both schemes is limited by the filter. To increase the tunability of the structure, a scheme composed of a PDM-MZM and a PolM [19] is proposed, but the scheme is not flexible in selecting the frequency of the generated signal.

In this paper, we propose a novel photonic scheme that can generate multiple formats of binary modulated signals. Only one modulator is used in the scheme, the structure is simple. The binary coding signal and the local oscillator (LO) signal are directly loaded on different RF ports of the dual-polarization quadrature phase shift-keying (DP-QPSK) modulator, the frequency and the data rate can be easily tuned. No filter or 90° HC is used in the scheme, the tuning range is large. Different modulation formats, such as ASK, FSK and PSK, can be obtained by properly setting the amplitude of the binary coding signal. The use of balanced photodetector (BPD) can effectively eliminate even harmonics and generate high-quality microwave signals.

2. Principles

Fig. 1 illustrates the structure of proposed binary modulated microwave signals generator. It consists of an LD, a DP-QPSK modulator, a polarization controller (PC), a polarization beam splitter (PBS), and a BPD. A linearly polarized optical signal from an LD is sent to the DP-QPSK modulator via a PC. The LO signal and a binary-coding signal are applied to the DP-QPSK modulator. Through setting the bias voltages properly, the DP-QPSK modulator outputs a polarization-multiplexed signal, the optical carrier modulated by the coding signal and the ±1 order sidebands are orthogonal in polarization. The polarization-multiplexed signal is then injected into the PBS through a PC. By adjusting the PC, the sum of the polarization-multiplexed signals and the difference between the polarization-multiplexed signals are respectively aligned with the two axes of the PBS. The two

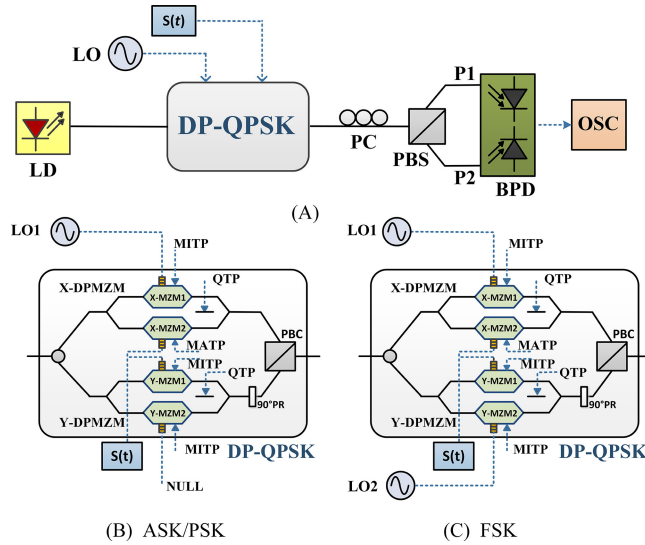


Fig. 1. Schematic diagram of the proposed binary modulated microwave signals generator. LD: laser diode; DP-QPSK: dual-polarization quadrature phase-shift keying modulator; 90° PR: 90° polarization rotator; PC: polarization controller; PBS: polarization beam splitter; BPD: balanced photodetector; LO: Local oscillator; OSC: oscilloscope; MATP: maximum transmission point; MITP: minimum transmission point; QTP: quadrature transmission point.

outputs of the PBS are separately injected into the BPD to obtain the desired binary modulated signals.

As described in Fig. 1, a DP-QPSK modulator consists of a Y-splitter, two parallel dual-parallel Mach-Zehnder modulators (X-DPMZM and Y-DPMZM), a 90° polarization rotator (90° PR), and a polarization beam combiner (PBC). We assume that the optical carrier from the LD is $E_{in}(t) = E_0 \exp(j\omega_c t)$, where E_0 and ω_c are the amplitude and angular frequency of the optical carrier. Assume that the binary coded signal loaded on the DP-QPSK modulator is $s(t)$. Two LO signals (LO_1 and LO_2) are expressed as $V_{LO_1}(t) \sin(\omega_{LO_1} t)$ and $V_{LO_2}(t) \sin(\omega_{LO_2} t)$, respectively, where V_{LO_1} and V_{LO_2} are the amplitudes, ω_{LO_1} and ω_{LO_2} are the angular frequencies. The modulation indexes (m_{LO_1} and m_{LO_2}) for LO_1 and LO_2 can be written as $m_{LO_1} = \pi V_{LO_1}/V_\pi$ and $m_{LO_2} = \pi V_{LO_2}/V_\pi$, respectively, where V_π is the half-wave voltage of the DP-QPSK modulator.

2.1 Generation of ASK and PSK signals

As shown in Fig. 1 (b), the binary coding signal $s(t)$ is divided into two equal parts by a power splitter and loaded on X-MZM2 and Y-MZM1, respectively. The RF port of X-MZM1 is loaded with LO_1 and the RF port of Y-MZM2 is null. The two sub-modulators and the main modulator of X-DPMZM are biased at MITP, MATP and QTP, respectively. And the two sub-modulators and main modulator of Y-DPMZM are biased at the MITP, MITP and QTP, respectively. The polarization-multiplexed signal from the DP-QPSK modulator is described as:

$$\begin{aligned} E_{DP_QPSK}(t) &= E_{X_DPMZM}(t) + E_{Y_DPMZM}(t) \\ &= \frac{\sqrt{2}E_{in}(t)}{8} \left(\left\{ (\exp[jm_{LO_1} \sin(\omega_{LO_1} t) + j\pi/2] + \exp[-jm_{LO_1} \sin(\omega_{LO_1} t) - j\pi/2]) \right\} \vec{e}_x \right. \\ &\quad \left. + \left\{ (\exp[j\beta s(t)] + \exp[-j\beta s(t)]) \exp(j\pi/2) \right. \right. \\ &\quad \left. \left. + \{\exp[j\beta s(t) + j\pi/2] + \exp[-j\beta s(t) - j\pi/2]\} \vec{e}_y \right\} \right) \quad (1) \\ &\propto E_0 \exp(j\omega_0 t) \left\{ [-J_1(m_{LO_1}) \sin(\omega_{LO_1} t) + j \cos(\beta s(t))] \vec{e}_x - \sin(\beta s(t)) \vec{e}_y \right\} \end{aligned}$$

where \vec{e}_x and \vec{e}_y represent two orthogonal polarization states, respectively. $\beta = \pi V_{s(t)}/V_\pi$ is the modulation index of $s(t)$, $V_{s(t)}$ is the amplitude of the binary coding signal $s(t)$. $J_n(\bullet)$ represents the

n-order Bessel function of the first kind. Under small-signal assumption in the above equations, only the first-order optical sidebands are considered and higher-order sidebands are ignored.

The polarization-multiplexed signal from the DP-QPSK modulator is fed into the PBS via a PC. The cascaded PC and PBS can achieve polarization direction rotation. By carefully turning the PC, the angle between the polarization direction of one polarization of the polarization-multiplexed signal and the main-axis of PBS is 45 degrees. The phase difference between X and Y polarization states is 0 degrees. The two polarization-multiplexed signals at the output of the PBS can be denoted as:

$$\begin{aligned} & \begin{bmatrix} E_{P1}(t) \\ E_{P2}(t) \end{bmatrix} = T_{PC-PBS} \begin{bmatrix} E_{X-DPMZM}(t) \\ E_{Y-DPMZM}(t) \end{bmatrix} \\ &= \begin{bmatrix} \cos \alpha & -\sin \alpha \exp(j\theta) \\ \sin \alpha \exp(j\theta) & \cos \alpha \end{bmatrix} \begin{bmatrix} E_{X-DPMZM}(t) \\ E_{Y-DPMZM}(t) \end{bmatrix} \\ &= \begin{bmatrix} E_{X-DPMZM}(t) \cos \alpha - E_{Y-DPMZM}(t) \sin \alpha \exp(j\theta) \\ E_{X-DPMZM}(t) \sin \alpha \exp(j\theta) + E_{Y-DPMZM}(t) \cos \alpha \end{bmatrix} \\ &\propto E_0 \exp(j\omega_0 t) \begin{bmatrix} j \exp[-j\beta s(t)] - J_1(m_{LO_1}) \sin(\omega_{LO_1} t) \\ j \exp[j\beta s(t)] - J_1(m_{LO_1}) \sin(\omega_{LO_1} t) \end{bmatrix} \end{aligned} \quad (2)$$

where $\alpha = 45^\circ$ and $\theta = 0^\circ$ are introduced by PC.

Two output signals of the PBS are sent to BPD. After photodetection, the resulting electric signal can be denoted as:

$$\begin{aligned} I_{BPD} &= E_{P1}(t)E_{P1}^*(t) - E_{P2}(t)E_{P2}^*(t) \\ &= E_0^2 \left\{ \begin{array}{l} \underbrace{1}_{DC} + \underbrace{J_1^2(m_{LO_1}) \sin^2(\omega_{LO_1} t)}_{Harmonics} \\ - \underbrace{j J_1(m_{LO_1}) \sin(\omega_{LO_1} t) \exp[-j\beta s(t)] + j J_1(m_{LO_1}) \sin(\omega_{LO_1} t) \exp[j\beta s(t)]}_{ASK/PSK} \\ - \underbrace{1}_{DC} + \underbrace{J_1^2(m_{LO_1}) \sin^2(\omega_{LO_1} t)}_{Harmonics} \\ - \underbrace{j J_1(m_{LO_1}) \sin(\omega_{LO_1} t) \exp[j\beta s(t)] + j J_1(m_{LO_1}) \sin(\omega_{LO_1} t) \exp[-j\beta s(t)]}_{ASK/PSK} \end{array} \right\} \\ &= E_0^2 \{2 j J_1(m_{LO_1}) \sin(\omega_{LO_1} t) (\exp[j\beta s(t)] - \exp[-j\beta s(t)])\} \\ &= -4 E_0^2 J_1(m_{LO_1}) \sin(\omega_{LO_1} t) \sin[\beta s(t)] \end{aligned} \quad (3)$$

It can be seen from Eq. (3), due to the balanced detection of the BPD, the undesired terms such as DC and harmonics are effectively eliminated and a better quality ASK or PSK signal is generated. By properly adjusting the amplitude $s(t)$, when $\beta s(t) = 0$ at bit '0' and $\beta s(t) = \pi/2$ at bit '1', the ASK signal is generated. The expression can be written as:

$$\begin{aligned} I_{BPD} &\propto J_1(m_{LO_1}) \sin(\omega_{LO_1} t) \sin[\beta s(t)] \\ &= \begin{cases} 0 & \text{for bit '0'} \\ J_1(m_{LO_1}) \sin(\omega_{LO_1} t) & \text{for bit '1'} \end{cases} \end{aligned} \quad (4)$$

Similarly, if the binary coding signal $s(t)$ satisfies the expression $\beta s(t) = -\pi/2$ at bit '0' and $\beta s(t) = \pi/2$ at bit '1', the output signal becomes an PSK signal, and the expression can be expressed as:

$$\begin{aligned} I_{BPD} &\propto J_1(m_{LO_1}) \sin(\omega_{LO_1} t) \sin[\beta s(t)] \\ &= \begin{cases} J_1(m_{LO_1}) \sin(\omega_{LO_1} t + \pi) & \text{for bit '0'} \\ J_1(m_{LO_1}) \sin(\omega_{LO_1} t) & \text{for bit '1'} \end{cases} \end{aligned} \quad (5)$$

2.2 Generation of FSK signal

As shown in Fig. 1 (c), two different LO signals (LO_1 and LO_2) are loaded on X-MZM1 and Y-MZM2, respectively. The X-MZM2 and Y-MZM1 are driven by the binary coding signal $s(t)$. The bias voltage setting of the DP-QPSK modulator is the same as that of ASK / PSK signal generation. And the polarization-multiplexed signal output from DP-QPSK modulator is written as:

$$\begin{aligned} E_{DP_QPSK}(t) &= E_{X_DPMZM}(t) + E_{Y_DPMZM}(t) \\ &= \frac{\sqrt{2}E_{in}(t)}{8} \left(\begin{array}{l} \left\{ \begin{array}{l} \left[\exp(jm_{LO_1} \sin(\omega_{LO_1} t) + j\pi/2) \right] \\ + \exp(-jm_{LO_1} \sin(\omega_{LO_1} t) - j\pi/2) \end{array} \right\} \vec{e}_x \\ + \left\{ \begin{array}{l} [\exp(j\beta s(t)) + \exp(-j\beta s(t))] \exp(j\pi/2) \\ + [\exp(j\beta s(t) + j\pi/2) + \exp(-j\beta s(t) - j\pi/2)] \end{array} \right\} \vec{e}_y \\ + \left\{ \begin{array}{l} \left[\exp(jm_{LO_2} \sin(\omega_{LO_2} t) + j\pi/2) \right] \exp(-j\pi/2) \\ + \left[\exp(-jm_{LO_2} \sin(\omega_{LO_2} t) - j\pi/2) \right] \end{array} \right\} \vec{e}_y \\ \propto \left\{ -J_1(m_{LO_1}) \sin(\omega_{LO_1} t) + j \cos[\beta s(t)] \right\} \vec{e}_x + \left\{ -\sin[\beta s(t)] + j J_1(m_{LO_2}) \sin(\omega_{LO_2} t) \right\} \vec{e}_y \end{array} \right) \end{aligned} \quad (6)$$

As mentioned above, by adjusting the PC to meet $\alpha = 45^\circ$ and $\theta = 0^\circ$, the optical signal output from the PBS is described as:

$$\begin{aligned} \begin{bmatrix} E_{P1}(t) \\ E_{P2}(t) \end{bmatrix} &= \begin{bmatrix} E_{X_DPMZM}(t) + E_{Y_DPMZM}(t) \\ E_{X_DPMZM}(t) - E_{Y_DPMZM}(t) \end{bmatrix} \\ &= \begin{bmatrix} j \cos[\beta s(t)] - J_1(m_{LO_1}) \sin(\omega_{LO_1} t) + j J_1(m_{LO_2}) \sin(\omega_{LO_2} t) - \sin[\beta s(t)] \\ j \cos[\beta s(t)] - J_1(m_{LO_1}) \sin(\omega_{LO_1} t) - j J_1(m_{LO_2}) \sin(\omega_{LO_2} t) + \sin[\beta s(t)] \end{bmatrix} \end{aligned} \quad (7)$$

Next, the two output signals from PBS are injected into the BPD. The resulting electrical signal is given by

$$\begin{aligned} I_{BPD} &= E_{P1}(t)E_{P1}^*(t) - E_{P2}(t)E_{P2}^*(t) \\ &\propto J_1(m_{LO_1}) \sin(\omega_{LO_1} t) \sin[\beta s(t)] + J_1(m_{LO_2}) \sin(\omega_{LO_2} t) \cos[\beta s(t)] \end{aligned} \quad (8)$$

The amplitude condition for the generation of FSK signal is that the expression $\beta s(t) = 0$ at bit '0' and $\beta s(t) = -\pi/2$ at bit '1'. To obtain a flat waveform, the amplitude of the input LO signals should introduce the same modulation index, i.e., $m_{LO_1} = m_{LO_2} = m$. Then, we can rewrite Eq. (8) as:

$$\begin{aligned} I_{BPD} &= E_{P1}(t)E_{P1}^*(t) - E_{P2}(t)E_{P2}^*(t) \\ &\propto J_1(m) \{ \sin(\omega_{LO_2} t) \cos[\beta s(t)] + \sin(\omega_{LO_1} t) \sin[\beta s(t)] \} \\ &= \begin{cases} J_1(m) \sin(\omega_{LO_2} t) , \text{ for bit '0'} \\ J_1(m) \sin(\omega_{LO_1} t) , \text{ for bit '1'} \end{cases} \end{aligned} \quad (9)$$

It can be seen from Eq. (9) that the coding signal $s(t)$ determines the frequency of the FSK signal. The bit '0' and '1' corresponds to an instantaneous LO frequency of ω_{LO_2} and ω_{LO_1} , respectively.

3. Experiments and Results

3.1 Experimental Setup

To verify the feasibility of the proposed scheme, a proof-of-concept experiment of binary modulated microwave signal generation is carried out as shown in Fig. 1(a). A distributed feedback LD (Emcore 1782) is used as the continuous-wave light source, which emits linearly polarized light with the wavelength of around 1551.1 nm, the power of 12 dBm, and the RIN of -150 dBc/Hz. Then it is injected into a DP-QPSK modulator (Fujitsu, FTM7977EX) via a PC. The half-wave voltage of the DP-QPSK modulator is 3.5 V, and the insertion loss and extinction ratio are 13 dB and 25 dB, respectively. Two microwave analog signal generators (MSGs, R&S SMW 200A and Agilent N5183A MXG) are used to offer LO signals (LO_1 and LO_2). A pseudo-random binary sequence (PRBS) signal generated by an arbitrary waveform generator (AWG, Tektronix AWG7082) is used as the binary coding signal $s(t)$. The LO signals and the binary coding signal $s(t)$ are respectively loaded on different RF ports of the DP-QPSK modulator. The optical signal from DP-QPSK

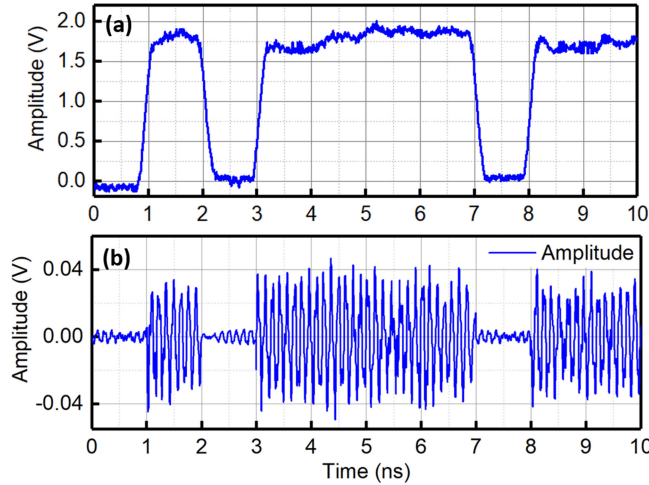


Fig. 2. Waveform of (a) the binary coding signal $s(t)$ loaded on DP-QPSK modulator and (b) the generated 1-Gbps 8-GHz ASK signal.

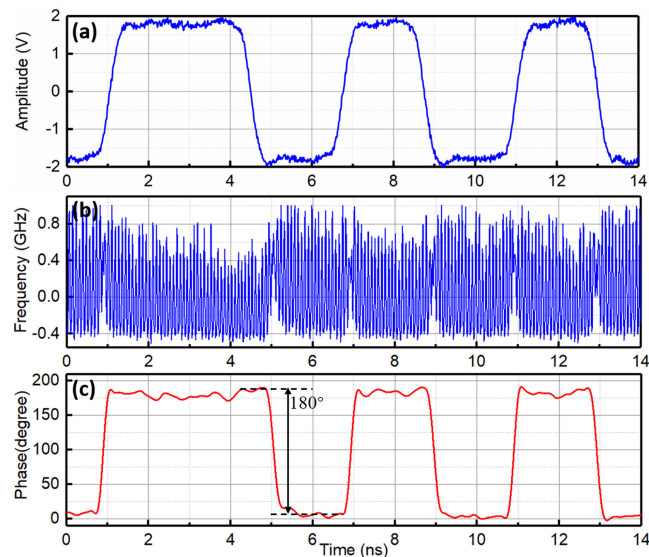


Fig. 3. The waveform of the binary coding signal $s(t)$ used to produce phase shift keying (PSK) signal is shown in (a). (b) The waveform of the generated 0.5-Gbps 12-GHz PSK and (c) the corresponding recovered phase.

modulator is injected into the BPD (Finisar XPDV 2150R) through the PC and the PBS, and the optical signal is converted into an electrical signal by a BPD. The bandwidth and responsivity of the BPD is 50 GHz and 0.6 A/W, respectively. We used an optical spectrum analyzer (Advantest, Q8384) to monitor the optical signal and an electrical spectrum analyzer (ESA, Rohde & Schwarz, FSW30) to observe the generated electrical signal. The temporal waveform is monitored by an oscilloscope (Keysight DSOV334A) with a sampling rate of 80 GSa/s.

3.2 Generation of ASK and PSK signals

An LO signal (LO_1) with a frequency of 8 GHz and a power of 14 dBm is loaded onto X-MZM1, which is biased at the MITP. Y-MZM2 is unloaded and the main modulator of Y-DPMZM is biased

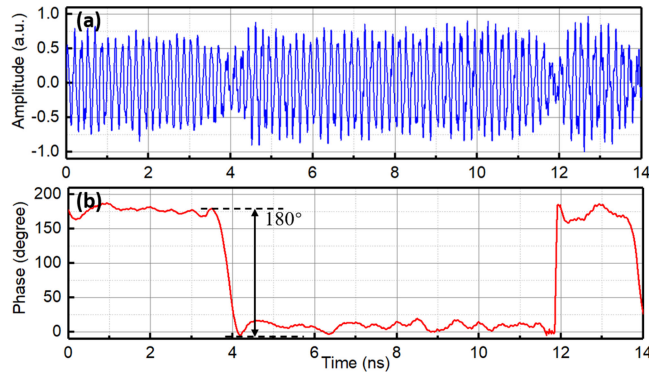


Fig. 4. (a) The waveform of the generated 0.5-Gbit/s 6-GHz PSK signal and (b) the corresponding recovered phase.

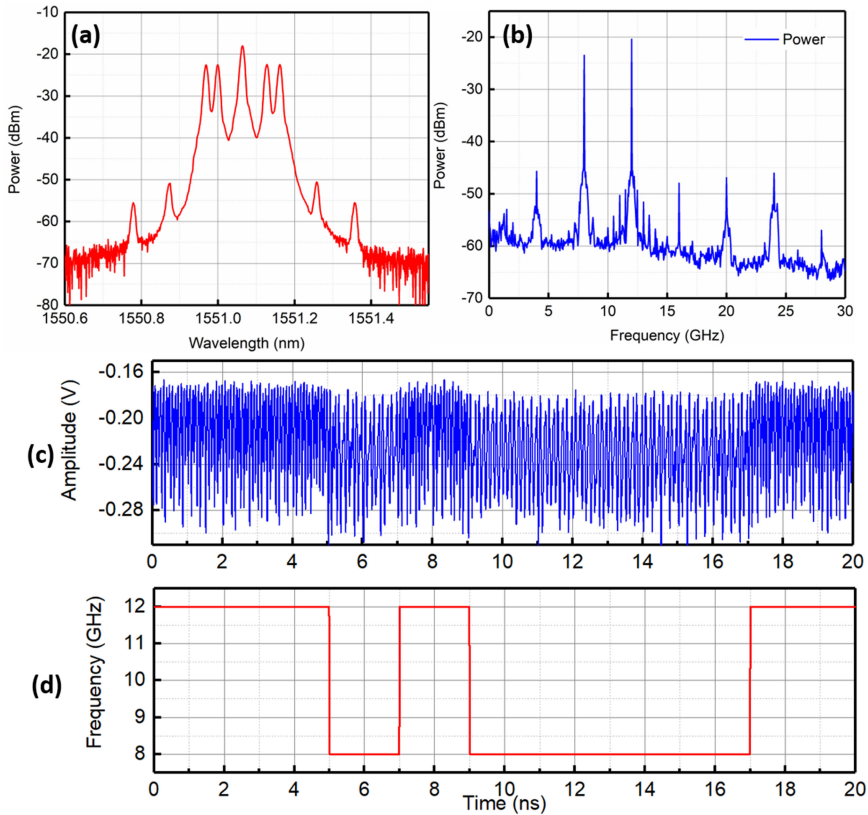


Fig. 5. (a) The spectra of the polarization-multiplexed signal output by the DP-QPSK modulator, (b) The electrical spectrum of the generated FSK signal, (c) The waveform, and (d) corresponding frequency.

at the QTP. A binary coding signal $s(t)$ with a length of $2^{13}-1$ bits and a rate of 1 Gbps is loaded on X-MZM2 and Y-MZM1 by a power splitter. The working points of X-MZM2 and Y-MZM1 are biased at the MATP and the MITP, respectively. The waveform of binary coding signal $s(t)$ is shown in Fig. 2(a), where the amplitude of it at bit '1' and bit '0' are about 1.75 V and 0 V, respectively. Fig. 2(b) is the real-time waveform diagram of microwave ASK signal, in which the modulation rate is 1 Gbps and carrier frequency is 8 GHz.

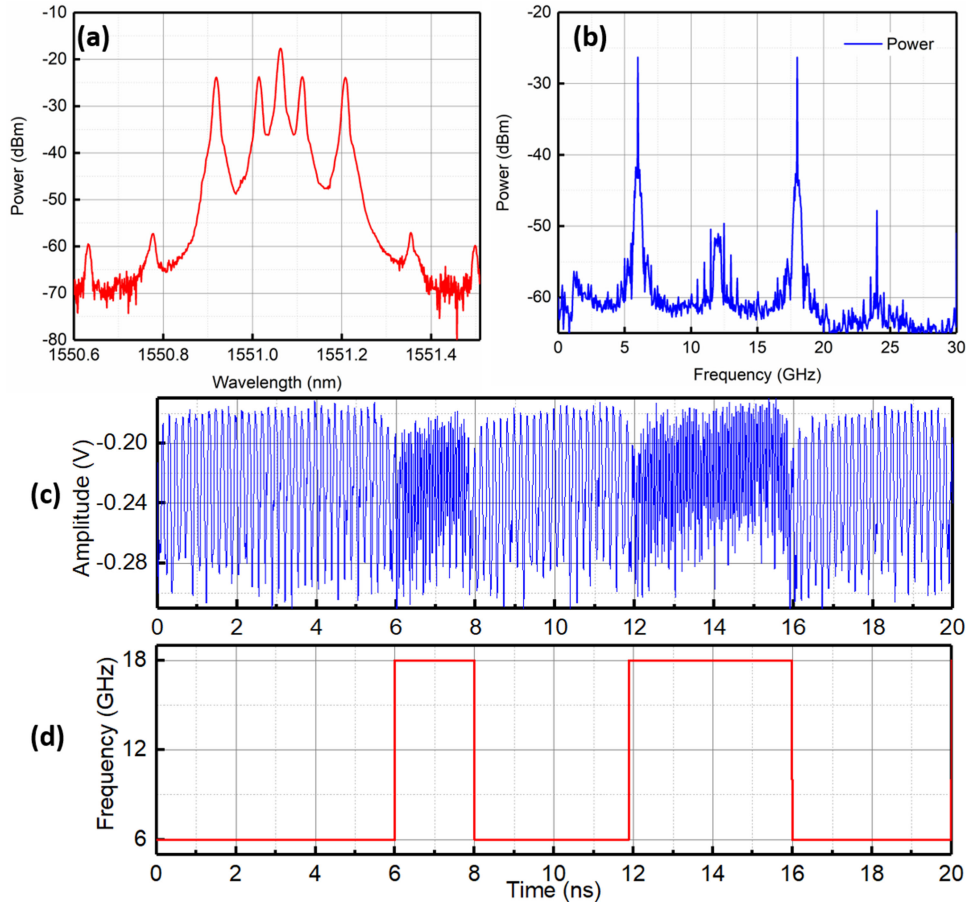


Fig. 6. (a) The spectra of the polarization-multiplexed signal output by the DP-QPSK modulator, (b) The electrical spectrum of the generated FSK signal, (c) The waveform, and (d) corresponding frequency.

Keeping the bias voltages of the DP-QPSK modulator unchanged, we change the amplitude of the binary coding signal $s(t)$ to 1.75 V at bit 1 and -1.75 V at bit 0. Limited by the AWG bandwidth, the data rate is set to 0.5 Gbps. The frequency of LO_1 is changed to 12 GHz. The output signal changes from ASK signal to PSK signal. The waveform of the binary coding signal $s(t)$ loaded on the DP-QPSK modulator is shown in Fig. 3 (a), the symbol sequence is PRBS signals, and the data rate is 0.5 Gbps. The blue line in Fig. 3(b) denotes the temporal waveforms of the PSK signal, it can be seen that there are obvious phase jumps between different symbols. The red line in Fig. 3(c) is the phase information recovered after off-line processing of PSK signal [20]. It can be observed from the figure that the phase difference of different symbols is approximately equal to 180 degrees, which is consistent with the input binary sequence.

In order to verify the tunability of the proposed system, the frequency of the input LO signal is changed to 6 GHz. The time domain waveform of the generated PSK signal is shown by the blue line in Fig. 4. The red line is the phase information recovered from the PSK signal by Hilbert transform, which is close to the theoretical value.

3.3 Generation of FSK signal

As described in Fig. 1(c), two LO signals (LO_1 and LO_2) with a frequency of 8 GHz and 12 GHz, and a power of 14 dBm are loaded on the DP-QPSK modulator. It should be noted that the bias

voltages of DP-QPSK modulator remain unchanged. In the FSK signal generation experiment, the amplitude setting of binary coded signal $s(t)$ is the same as that of ASK signal generation. We adjust the amplitude of the binary coded signal $s(t)$ to 1.75 V at bit '1' and 0 V at bit '0', and the rate is set to 0.5 Gbps. The spectra of polarization-multiplexed signal is plotted in Fig. 5 (a). Similar to ASK/PSK signal generation, a 45-degrees angle is introduced between the polarization direction of the polarization-multiplexed signal and the main axis of the PBS. Then the two output signals from the PBS are injected into a BPD to generate an FSK signal.

The electrical spectrum and time-domain waveforms are plotted in Fig. 5 (b) and Fig. 5 (c), respectively. Due to the balance detection of BPD, there are few spurs in the electrical spectrum, and the generated FSK signal waveform has little fluctuation. We use the coherent demodulation algorithm of MATLAB to recover the frequency information of the received signal, as shown by the red line in Fig. 5 (d). It can be seen from the figure that the frequency of the generated FSK signal jumps between 8 GHz and 12 GHz.

To investigate the tunability of the FSK signal, we change the frequency of the microwave signals (LO_1 and LO_2) at 6 GHz and 18 GHz and keeping the other parameters of the scheme unchanged. The corresponding optical spectrum of polarization-multiplexed signal is measured by the optical spectrum analyzer and illustrated in Fig. 6 (a). It can be seen from the electrical spectrum shown in Fig. 6(b) that the two subcarrier frequencies of the generated FSK signal are 6 GHz and 18 GHz. In Fig. 6 (c), the blue line depicts the temporal waveform of the generated FSK signal, while the red line in Fig. 6 (d) represents the frequency value recovered by the coherent demodulation algorithm of MATLAB.

4. Conclusion

In conclusion, a novel microwave binary modulated signal generator is proposed and experimentally verified. The structure can flexibly generate three binary modulation formats. PSK or ASK signal can be generated by adjusting the amplitude of the binary coding signal. Loading two different LO signals on the DP-QPSK modulator and keeping the other parameters unchanged, we can change the modulation format from ASK to FSK. Since the two LO signals are loaded on different RF ports of the DP-QPSK modulator, the two LO frequencies can be tuned flexibly in large range. Compared with traditional electronic methods, the proposed photonic binary modulation signal generator has a simpler structure, a larger working bandwidth, and better immunity to electromagnetic interference. When the carrier frequency of the modulated signal is lower than 10 GHz, optical fiber transmission with a length of less than 10 km can be used with little power fading. If high carrier frequency modulated signals are required for long-distance transmission, negative dispersion devices need to be used to compensate for fiber dispersion [21].

References

- [1] P. Ghelfi *et al.*, "A fully photonics-based coherent radar system," *Nature*, vol. 507, no. 7492, pp. 341–345, Mar. 2014.
- [2] M. K. Simon *et al.*, *Spread Spectrum Communications Handbook*. New York, NY, USA: McGraw-Hill, 1994.
- [3] J. Capmany and D. Novak, "Microwave photonics combines two worlds," *Nat. Photon.*, vol. 53, no. 6, pp. 319–331, Jun. 2007.
- [4] J. Yao, "Microwave photonics," *J. Lightw. Technol.*, vol. 27, no. 3, pp. 314–335, Feb. 2009.
- [5] J. D. McKinney, D. E. Leaird, and A. M. Weiner, "Millimeter-wave arbitrary waveform generation with a direct space-to-time pulse shaper," *Opt. Lett.*, vol. 27, no. 15, pp. 1345–1347, Aug. 2002.
- [6] J. Ye *et al.*, "Photonic generation of microwave phase-coded signals based on frequency-to-time conversion," *IEEE Photon. Technol. Lett.*, vol. 24, no. 17, pp. 31527–31529, Jul. 2012.
- [7] Y. Long, L. Zhou, and J. Wang, "Photonic-assisted microwave signal multiplication and modulation using a silicon Mach-Zehnder modulator," *Sci. Rep.*, vol. 6, no. 1, Feb. 2016, Art. no. 20215.
- [8] P. Ghelfi, F. Scotti, F. Laghezza, and A. Bogoni, "Phase coding of RF pulses in photonics-aided frequency-agile coherent radar systems," *IEEE J. Quantum Electron.*, vol. 48, no. 9, pp. 1151–1157, Sep. 2012.
- [9] W. Li *et al.*, "Photonic generation of arbitrarily phase-modulated microwave signals based on a single DDMZM," *Opt. Exp.*, vol. 22, no. 7, pp. 7446–7457, Apr. 2014.
- [10] M. Lei *et al.*, "Photonic generation of background-free binary and quaternary phase-coded microwave pulses based on vector sum," *Opt. Exp.*, vol. 27, no. 15, pp. 20774–20784, Jul. 2019.

- [11] S. Zhu *et al.*, "Simultaneous frequency upconversion and phase coding of a radio-frequency signal for photonic radars," *Opt. Lett.*, vol. 43, no. 3, pp. 583–586, Feb. 2018.
- [12] L. Gao, X. Chen, and J. Yao, "Photonic generation of a phase-coded microwave waveform with ultrawide frequency tunable range," *IEEE Photon. Technol. Lett.*, vol. 25, no. 10, pp. 899–902, May 2013.
- [13] Y. Yu, J. Dong, F. Jiang, and X. Zhang, "Photonic generation of precisely π phase-coded microwave signal with broadband tunability," *IEEE Photon. Technol. Lett.*, vol. 25, no. 24, pp. 2466–2469, Dec. 2013.
- [14] J. Ye, L. Yan, H. Chen, W. Pan, B. Luo, and X. Zou, "Photonic generation of microwave frequency shift keying signal using a polarization maintaining FBG," *IEEE Photon. J.*, vol. 10, no. 3, Jun. 2017, Art. no. 5501108.
- [15] Y. Chen, "High-speed and wideband frequency-hopping microwave signal generation via switching the bias point of an optical modulator," *IEEE Photon. J.*, vol. 10, no. 1, Feb. 2018, Art. no. 5500407.
- [16] L. Huang *et al.*, "Photonic generation of microwave frequency shift keying signals," *IEEE Photon. Technol. Lett.*, vol. 28, no. 18, pp. 1928–1931, Sep. 2016.
- [17] P. Xiang *et al.*, "A novel approach to photonic generation of RF binary digital modulation signals," *Opt. Exp.*, vol. 21, no. 1, pp. 631–639, Jan. 2013.
- [18] X. Feng *et al.*, "Photonic generation of RF binary digitally modulated signals," *Opt. Exp.*, vol. 25, no. 16, pp. 19043–19051, Aug. 2017.
- [19] K. Zhang *et al.*, "Reconfigurable photonic generation of background-free microwave waveforms with multi-format," *Opt. Commun.*, vol. 453, Aug. 2019, Art. no. 124326.
- [20] S. Zhu, M. Li, X. Wang, N. H. Zhu, and Z. Cao, "Photonic generation of background-free binary phase-coded microwave pulses," *Opt. Lett.*, vol. 44, no. 1, pp. 94–97, Jan. 2019.
- [21] H. Sun, M. C. Cardakli, and K. M. Feng, "Tunable RF-power-fading compensation of multiple-channel double-sideband SCM transmission using a nonlinearly chirped FBG," *IEEE Photon. Technol. Lett.*, vol. 12, no. 5, pp. 546–548, May 2000.